Journal of Power Sources 245 (2014) 779–786

Contents lists available at SciVerse ScienceDirect

Journal of Power Sources

journal homepage: www.elsevier.com/locate/jpowsour

# Poly(vinylidene fluoride)-based, co-polymer separator electrolyte membranes for lithium-ion battery systems

C.M. Costa [a], J.L. Gomez Ribelles [b,c], S. Lanceros-Méndez [a,d,*], G.B. Appetecchi [e,**], B. Scrosati [e]

[a] Center/Department of Physics, University of Minho, 4710-057 Braga, Portugal
[b] Center for Biomaterials and Tissue Engineering, Universitat Politècnica de València, 46022 Valencia, Spain
[c] Networking Research Center on Bioengineering, Biomaterials and Nanomedicine (CIBER-BBN), Valencia, Spain
[d] INL – International Iberian Nanotechnology Laboratory, 4715-330 Braga, Portugal
[e] University of Rome "La Sapienza", P.le A. Moro 5, 00185 Rome, Italy

## HIGHLIGHTS

- Electrolyte membranes based on PVdF co-polymers hosts.
- Large liquid uptake with fast $Li^+$ ion transport properties.
- Very good cycling performance in LiFePO4 and Sn–C half-cells.

## ARTICLE INFO

*Article history:*
Received 11 April 2013
Received in revised form
21 May 2013
Accepted 17 June 2013
Available online 5 July 2013

*Keywords:*
Poly(vinylidene fluoride) copolymers
Polymeric blends
Gel polymer electrolytes
Lithium battery applications

## ABSTRACT

In the present paper we report and discuss the physicochemical properties of novel electrolyte membranes, based on poly(vinylidenefluoride-co-trifluoroethylene), PVdF-TrFE, and poly(vinylidenefluoride-co-hexafluoropropylene), PVdF-HFP, co-polymer hosts and the PVdF-TrFE/poly(ethylene oxide (PEO) blend as separators for lithium battery systems. The results have shown that the examined separator membranes, particularly those based on the PVdF co-polymers, are able to uptake large liquid amounts leading to high ionic conductivity values.

Tests performed on Li/$LiFePO_4$ and Li/Sn–C cells have revealed very good cycling performance even at high current rates and 100% of DOD, approaching the results achieved in liquid electrolytes. A capacity fading lower than 0.002% per cycle was observed. Particularly, the Li/$LiFePO_4$ cathode cells have exhibited excellent rate capability, being still able to deliver at 2C above 89% of the capacity discharged at 0.1C. These results, in conjunction with the about 100% coulombic efficiency, suggest very good electrolyte/electrode compatibility, which results from the high purity and stability of the electrolyte and electrode materials and the cell manufacturing.



## 1. Introduction

Lithium-ion batteries are the most widely used energy storage systems for portable electronic devices such as cellular phones, notebook, camera, etc. [1,2]. In comparison to other technologies such as Ni–MH, it presents improvements in several characteristics, including weight (light), cost (cheap), energy density (high), no memory effect, prolonged service-life, electrochemical stability and high charge/discharge cycling performance [3]. Specific energy, power, safety and reliability are the most important issues related to the lithium-ion technology for batteries systems [4,5]. The basic components of a Li-ion battery are the anode, cathode and the electrolyte separator [6].

The development of new materials for cathodes, anodes and separators through the use of nano-structured materials as well as the optimization of cell design increases the power and energy (gravimetrical and volumetric) of lithium-ion battery systems without depleting their safety [7–9]. Anodes based on tin (Sn) nano-particles, obtained by dispersing nano-Sn in a carbon matrix (Sn–C), are very attractive for battery applications due to their large

* Corresponding author. Center/Department of Physics, University of Minho, 4710-057 Braga, Portugal. Tel.: +351 253 604 073; fax: +351 253 678 981.
** Corresponding author.
*E-mail addresses:* lanceros@fisica.uminho.pt (S. Lanceros-Méndez), gianni.appeteccchi@enea.it, gianni.appetecchi@alice.it (G.B. Appetecchi).

0378-7753/$ – see front matter © 2013 Elsevier B.V. All rights reserved.
http://dx.doi.org/10.1016/j.jpowsour.2013.06.151

theoretical capacity (993 mA h $g^{-1}$) [10–13] in comparison to conventional graphite (370 mA h $g^{-1}$) [1–6]. In addition, Sn–C anodes show good electrochemical performance in terms of lithium insertion/extraction and adequate mechanical stability [10–13].

The cathode materials with the orthorhombic olivine crystal structure such as lithium iron phosphate ($LiFePO_4$) are used in battery systems due to their excellent structural and thermal stability [14]. Main characteristics of $LiFePO_4$ are low cost, ability to run thousands of cycles without any appreciable degradation, high theoretical capacity (170 mA h $g^{-1}$) with a nominal voltage of 3.45 V *versus* the redox couple $Li/Li^+$ [14]. Due to its olivine structure, $LiFePO_4$ shows very flat charge/discharge plateau during the lithium cation intercalation/deintercalation process, good cycling stability and low electric conductivity (e.g., around $10^{-11}$ S $cm^{-1}$). Also, it is compatible with most existing organic electrolytes [15,16].

The electrolyte separator (e.g., a solution obtained by dissolving a suitable lithium salt in alkyl carbonate organic solvents), dividing the anode and the cathode in order to avoid short-circuit, serves as the medium for transferring the lithium ions from the anode to the cathode and *vice versa*. In order to improve the safety of the battery system and minimize liquid leakage [17,18], the electrolyte solution, constituted by volatile and flammable compounds, is incorporated in suitable polymeric matrices. The key properties/characteristics for separator membranes are thickness, permeability, porosity/pore size, wettability and chemical, thermal and mechanical stability [18–20]. The most investigated polymeric hosts as separator membranes are poly(ethylene), PE [21], poly(propylene), PP [22], poly(ethylene oxide), PEO [23–25], poly(acrylonitrile), PAN [26,27], poly(methylmethacrylate), PMMA [28], poly(vinylidenefluoride), PVdF, and its vinylidene fluoride, VdF, copolymers (PVdF-co-trifuoroethylene, PVdF-TrFE and PVdF-co-hexafluoropropylene, PVdF-HFP) [29–33].

PVdF and its copolymers exhibit adequate properties/characteristics such as high polarity (high dielectric constant), electron withdrawing fluorine atoms in the backbone structure, excellent thermal and mechanical properties, high affinity to electrolyte solutions, chemical inertness and stability in cathodic environment and controllable porosity in binary and ternary systems [34–36].

The copolymers of PVdF (PVdF-TrFE and PVdF-HFP) exhibit advantages with respect to the homopolymer ones and commercial PE battery separators. PVdF-HFP has low degree of crystallinity due to the addition of hexafluoropropylene (HFP), high mechanical flexibility and good compatibility with respect to electrodes [37,38]. PVdF-TrFE shows high dipole moment, high dielectric constant, and possibility of controlling porosity in the binary systems at room temperature [39]. The performance of PVdF-TrFE membranes for electrolyte battery applications has been studied as a function of the porosity, dehydration of lithium ions, and processing technique ($Li^+$ cation uptake vs. composite formation) and it was observed that these membranes are strongly influenced both by porosity and processing technique [39]. In addition, PVdF-TrFE-based electrolytes exhibit higher ionic conduction in comparison to commercial PE separators [32,40,41], resulting appealing as Li-ion battery separators. In addition, different co-monomers are expected to differently influence the physicochemical properties of the polymer electrolyte membranes, allowing improved performance to full batteries. One approach for increasing the properties of separator membranes is the fabrication of blend hosts to combine the characteristics of different polymeric materials. For instance, PVdF-TrFE/PEO polymer blends were realized in order to combine the good mechanical properties of PVdF with the high swelling capability of PEO in alkyl carbonate-based electrolyte solutions [25] to improve the solvation problems of PVdF-TrFE [42]. It was verified that microstructure, hydrophilicity and electrolyte uptake strongly depend on the PEO content within the blend [42].

In this work, we have investigated the physicochemical properties of electrolyte membranes based on the above mentioned PVdF co-polymer, e.g., PVdF-TrFE and PVdF-HFP, and blend separators, e.g., PVdF-TrFE/PEO, both in organic and non-volatile, non-flammable ionic liquid solutions. Also, the performance of the polymer electrolyte membranes was evaluated in $Li/LiFePO_4$ and Li/Sn–C half-cells.

## 2. Experimental

### 2.1. Materials

Poly(vinylidene fluoride-co-trifluoroethylene) (PVdF-TrFE, monomer mole ratio = 70/30, $M_w$ = 350,000 g $mol^{-1}$) and poly(vinylidene fluoride-co-hexafluoropropylene) (PVdF-HFP, 88/12, $M_w$ = 600,000 g $mol^{-1}$) were supplied from Solvay (Belgium). Poly(ethylene oxide) (PEO, $M_w$ = 100,000 g $mol^{-1}$) was purchased from Polysciences.

The organic electrolyte solution, e.g., 1 M lithium hexafluorophosphate ($LiPF_6$) in ethylene carbonate/dimethyl carbonate (EC–DMC, 1/1 in weight) was acquired from Merck (LP30, battery grade) and used as received. The ionic liquid electrolyte was a mixture of the lithium bis(trifluoromethanesulfonyl)imide, LiTFSI (purchased from Solvionic) salt with the ionic liquid *N*-butyl-*N*-methylpyrrolidinium bis(trifluoromethanesulfonyl)imide, $PYR_{14}TFSI$ (Solvionic). The LiTFSI/$PYR_{14}TFSI$ (mole ratio fixed equal to 1/9) mixture, prepared by dissolving the lithium salt in the ionic liquid compound, was successively vacuum dried (the vapor pressure of ionic liquids is non-detectable) overnight at 120 °C. Both the organic and ionic liquid electrolytes were stored and handled within a glove box (MBRAUN, moisture and oxygen level below 1 ppm).

### 2.2. Preparation of polymer separators and composite electrodes

PVdF-TrFE- and PVdF-HFP-based membranes were prepared by dissolving the polymer materials in *N*,*N*-dimethylformamide (DMF, from Merck) at a 15/85 polymer/solvent weight ratio.

Briefly, the copolymers were dissolved in the solvent (DMF) by room temperature magnetic stirring until a homogeneous and transparent solution was obtained. In order to prevent the formation of aggregates and to help the dissolution of the powders, the solution was hold 5 °C above room temperature for 15 min. Successively, the solution was kept, within a glass Petri dish, in a gas extraction chamber for 15 days (at room temperature) to allow DMF evaporation.

PVdF-TrFE/PEO (1/1 weight ratio) blends were prepared by dissolving the adequate amount of both polymer materials in DMF at a 15:85 polymer/solvent weight ratio [42]. The resulting solution was stirred at 60 °C for 4 h until to a homogeneous and transparent slurry was obtained. The latter was cast on a petri dish to allow the solvent removal (2 h at 70 °C) followed by vacuum drying for additional 3 h at 70 °C. Before testing, all separator membranes were dried under vacuum at 60 °C overnight and then transferred (within a sealed glass tube) into the glove box to avoid any contamination with the external atmosphere.

Composite electrodes were prepared by blending the active material ($LiFePO_4$ or Sn–C) (Sn:C weight ratio equal to 3:7 [43–46]), the electronic conductor (Super-P carbon, MMM) and the binder (PVdF, Solvay) in *N*-methyl-pyrrolidone. The so-obtained slurry was cast onto aluminum ($LiFePO_4$) or copper (Sn) foil, allowing the solvent removal. Coin electrodes, having a 10 mm diameter and thickness ranging from 40 μm to 50 μm, were punched from the tapes. Finally, the electrodes were dried under vacuum at 110 °C overnight and transferred in the glove box. The weight composition of electrodes resulted 80:10:10 with an active material mass loading of 3.0 mg $cm^{-2}$ (cathodes) and 4.6 mg $cm^{-2}$

(anodes). Taking into account for a reversible specific capacity of 170 mA h $g^{-1}$ ($LiFePO_4$) and 400 mA h $g^{-1}$ (Sn–C), this corresponds to 0.5 mA h $cm^{-2}$ ($LiFePO_4$) and 1.8 mA h $cm^{-2}$ (Sn), respectively.

### 2.3. SEM and DSC analysis

The morphology of the PVdF-based separator membranes was analyzed using a scanning electron microscopy (SEM) (Cambridge, Leica) with an accelerating voltage value equal to 15 kV. The membrane samples were coated with a very thin gold layer using a sputter coating (Polaron, model SC502 sputter coater). The samples, analyzed through their cross-section, were previously immersed in liquid nitrogen for 180 s and mechanically cut.

Differential scanning calorimetry (DSC) analysis was carried out with a Perkin–Elmer Pyris 1 DSC instrument under a nitrogen atmosphere flow between 25 and 200 °C at a heating rate of 10 °C $min^{-1}$. All samples were housed within the glove box in 30 μL aluminum pans with perforated lids to allow the release and removal of the decomposition products.

### 2.4. Liquid electrolyte uptake

The (open) porosity of the PVdF-based separator membranes was determined by He pycnometer. The physicochemical characterization of the PVdF-based separator membranes was performed within the glove box. The liquid electrolyte uptake was investigated by immersing the membrane under test in the $LiPF_6$–EC–DMC solution and recording the weight of the swollen sample (after removal of the solution excess on the membrane surface) as a function of the dipping time. The liquid content ($L_t$), achieved upon an immersion time equal to $t$, was evaluated by the following equation:

$$L_t = \left(1 - \left(\frac{M_0}{M_t}\right)\right) \times 100 \quad (1)$$

where $M_0$ is the mass of the pristine sample membrane and $M_t$ is the mass of the swollen membrane after immersion in the electrolyte solution. This test was run until to achieve a time-stable liquid uptake within the separator membrane. For the more viscous ionic liquid electrolyte (e.g., an excessive dipping time would be required for completely swelling the PVdF separators), the membrane samples were immersed in the $LiTFSI/PYR_{14}TFSI$ mixture and, then, transferred in the glove box vacuum chamber for 5 min to promote the full loading of the samples. The liquid uptake achieved upon 2 min dipping time was determined using Equation (1).

The electrolyte loss was determined by recording the weight variation of fully swollen sample membranes, exposed to the glove box atmosphere, as a function of the exposition time. The sample weight was normalized with respect to the initial one (e.g., fully swollen membrane). The test was not performed for the non-volatile ionic liquid electrolytes.

### 2.5. Cell manufacturing

All test cells were manufactured in the glove box. The ionic conductivity was investigated in 2032 coin-type cells with two stainless steel, blocking disk electrodes divided by a 400 μm PTFE circular spacer (having an internal area equal to 0.5 $cm^2$). The sample membrane (having a slightly higher thickness) was housed within the spacer.

The Li/$LiFePO_4$ and Li/Sn–C half-cells were fabricated by housing in 2032 coin-type containers the sequence composed by a lithium disc anode (10 mm diameter), a swollen PVdF-based membrane (14 mm) and a $LiFePO_4$ (or Sn–C) electrode (10 mm).

### 2.6. Electrochemical tests

The transport properties of the swollen membranes were determined by impedance spectroscopy measurements carried out at 25 °C and 50 °C on steel/membrane/steel symmetrical cells by applying a 10 mV alternate voltage in the 65 kHz–100 Hz frequency range using an Ametek VersaSTAT instrument. The ionic conductivity value ($\sigma$) was calculated through Equation (2):

$$\sigma = \frac{d}{R_b A} \quad (2)$$

where $R_b$ is the electrolyte bulk resistance, $d$ is the thickness and $A$ is the area of the membrane sample. The $R_b$ value was determined by fitting the AC responses using a Non-Linear Least-Square (NLLSQ) fit software [47,48] and defining an equivalent circuit, representing the electrochemical cell under study, which takes into account all possible contributes to the impedance of the tested electrolyte membranes [49,50].

The cycling performance of the Li/$LiFePO_4$ and Li/Sn–C half-cells was carried out using a multichannel Maccor 4000 battery tester at room temperature. The (galvanostatic) measurements were performed within the 2.0–4.0 V (cathode half-cells) and 0.01–2.0 V (anode half-cells) voltage range, respectively, at current rates from 0.1C through 2C.

## 3. Results and discussion

The swelling effect of the separator membrane size is evidenced in Fig. 1 which shows a picture of a PVdF-TrFE sample before (panel A) and after (panel B) immersing in $LiPF_6$–EC/DMC electrolyte solution. The loading with liquid electrolyte is witnessed by a slight increase in size of the sample and the turning of the membrane appearance from white to translucent. This latter behavior supports for interactions among the polymer chains and the solvent molecules. Also, the mechanical stability of the membranes is not influenced by the uptake processing, i.e., no fragmentation was observed.

The morphology of the PVdF separator membranes is presented in Fig. 2 (panels from A through C) as SEM images. The presence of open porosity with interconnected pathways is observed in all copolymer samples, being the pores smaller and dispersed in the blend samples. The porosity of the PVdF-TrFE (panel A) and PVdF-HFP (panel B) membranes is the result of the polymer–solvent

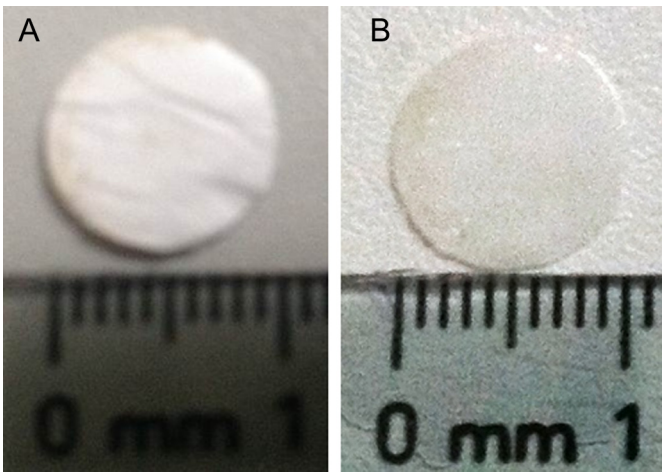


**Fig. 1.** Picture of a PVdF-TrFE membrane before (panel A) and upon (panel B) swelling in (1 M)$LiPF_6$–EC/DMC(1/1 in weight) electrolyte solution at room temperature.

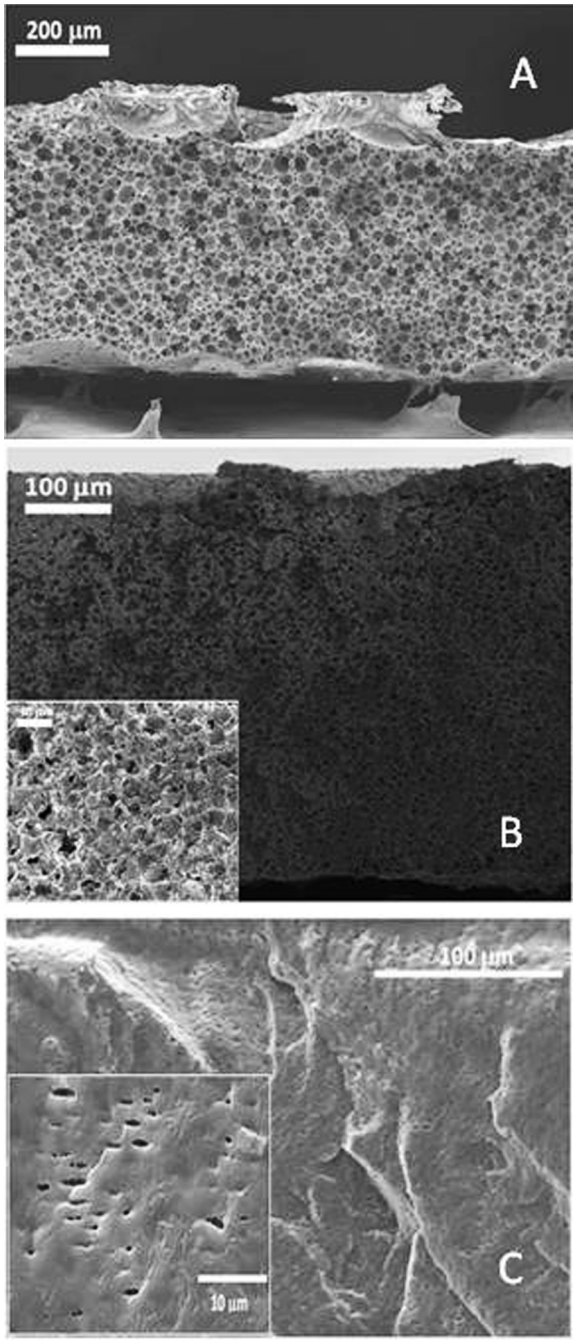


**Fig. 2.** Cross-section SEM images of different battery separator membranes. Panel A: PVdF-TrFE; panel B: PVdF-HFP; panel C: PVdF-TrFE/PEO. Magnifications are depicted in the insets.

interaction in the phase diagram of binary systems [51] and has been explained as a liquid–liquid phase separation and consequent crystallization of the copolymer rich phase [52]. For the PVdF-TrFE/PEO blend (panel C), the microstructure also is determined by the crystallization process, in which PEO polymer shows large spherulites (having a diameter larger than 50 µm, images not shown [42]). In panel C of Fig. 2 it is evidenced the roughness of the sample cross-sections, allowing to detect presence of crystalline PEO and small pores in the surface probably due to solvent evaporation (during drying at 70 °C). PVdF-TrFE crystallizes from solution during the drying process (70 °C), thus promoting diffusion of amorphous PEO chains through the porous structure [42].

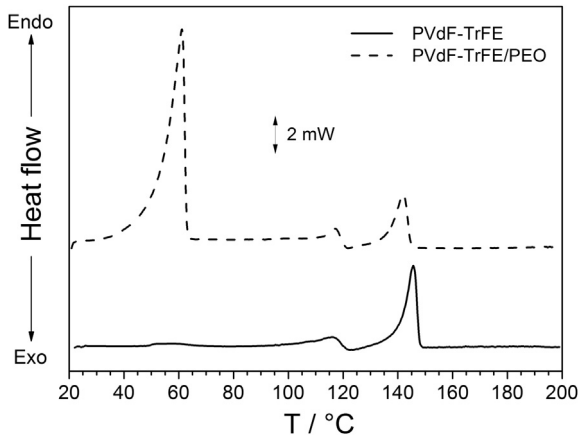


**Fig. 3.** DSC trace of selected electrolyte membranes based on different PVdF hosts. Scan rate: 10 °C $min^{-1}$.

The thermal behavior of selected membranes is reported as DSC traces in Fig. 3. For the PVdF-TrFE sample (solid line) two endothermic peaks are observed, the first one corresponding to the ferroelectric–paraelectric phase transition ($T_{FP}$) identified around 117 °C whereas the second one (145 °C) represents the melting temperature. The PVdF-HFP sample (data not reported) displays just one peak around 135 °C which corresponds to the fusion of the polymer. The DSC trace (dotted line) of the PVdF-TrFE/PEO blend evidences three peaks, the first one (around 61 °C) corresponding to the PEO melting and the other ones corresponding to the fusion of the PVdF-TrFE co-polymer.

The liquid electrolyte uptake vs. dipping time dependence is illustrated in Fig. 4 and summarized in Table 1. The PVdF-TrFE (panel A) and PVdF-HFP (panel B) membrane samples achieve saturation after approximately 6 min with a $LiPF_6$–EC–DMC content (with respect to the overall weight of the swollen membrane samples) equal to 84 wt.% and 81 wt.%, respectively, indicating that the (open) void volume was fully filled. Conversely, the PVdF-TrFE/PEO blend required much longer dipping times (1 h) to be saturated with a liquid electrolyte content not exceeding 45 wt.%. This larger necessary dipping time is to be attributed to the stronger interactions of the organic electrolyte (e.g., solvent molecules and lithium salt) with the PEO host compound. In addition, despite its

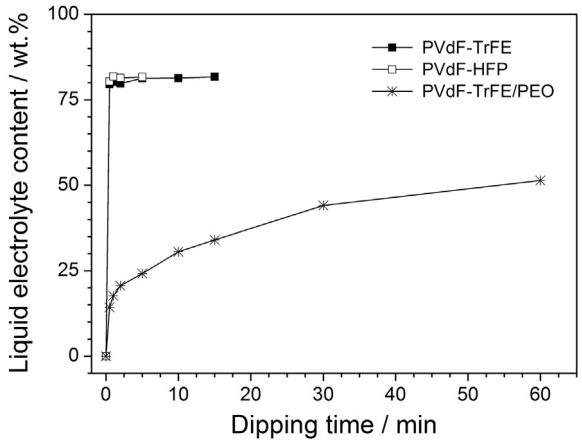


**Fig. 4.** Liquid electrolyte content vs. dipping time dependence (at room temperature) for $Li^+$-conducting, polymer membranes based on PVdF-TrFE (panel A), PVdF-HFP (panel B) and PVdF-TrFE/PEO (panel C) hosts during immersing in (1 M)$LiPF_6$–EC/DMC(1/1 in weight) electrolyte solution.

**Table 1**
Porosity, liquid content and ionic conductivity of electrolyte membranes based on different PVdF hosts. Organic = (1 M)$LiPF_6$ in EC/DMC (1/1 in weight) organic electrolyte. RTIL = (0.1)LiTFSI–(0.9)$PYR_{14}$TFSI ionic liquid electrolyte (0.1 and 0.9 represent the mole fractions).

| Polymer host | Porosity/% in volume | Liquid content/wt.% | | Conductivity (24 °C)/mS $cm^{-1}$ | | Conductivity (50 °C)/mS $cm^{-1}$ | |
|---|---|---|---|---|---|---|---|
| | | Organic | RTIL | Organic | RTIL | Organic | RTIL |
| PVdF-TrFE | 72 | 84 | 71 | 2.6 | 0.4 | 4.9 | 0.9 |
| PVdF-HFP | 60 | 81 | 75 | 3.5 | 0.4 | 4.8 | 1.2 |
| PVdF-TrFE/PEO | 30 | 45 | 24 | 2.3 | 0.006 | 3.8 | 0.015 |

swelling ability in alkyl carbonate-based electrolyte solutions [25], PEO is not allowed to largely swell when constricted in a blend with other polymeric materials (e.g., PVdF). The lower porosity exhibited by the PVdF-TrFE/PEO blends with respect to the neat PVdF-TrFE membranes is indicated by their less remarkable liquid uptake (Fig. 4).

The dipping tests in LiTFSI–$PYR_{14}$TFSI led to lower electrolyte content, e.g., 71 wt.%, 75 wt.% and 24 wt.% for PVdF-TrFE, PVdF-HFP and PVdF-TrFE/PEO, respectively, despite the higher density of the ionic liquid electrolyte (1.4 g $cm^{-3}$) with respect to the organic solution (1.2 g $cm^{-3}$), thus suggesting a lower wettability of the LiTFSI–$PYR_{14}$TFSI mixture toward the PVdF polymer hosts. The results of the swelling tests are in agreement with the porosity measurements (Table 1), which have shown higher void volume fraction for the PVdF co-polymer (72% and 60% for PVdF-TrFE and PVdF-HFP, respectively) with respect to the PVdF-TrFE/PEO blend (30%). This fact is strongly dependent on the membrane processing conditions [25,53].

In Fig. 5 it is displayed the weight variation (recorded at room temperature) as a function of the storage time (in glove box atmosphere) of the swollen PVdF-based separator membranes immediately after electrolyte uptake. An exponential decay in weight was detected for all investigated samples until leveling time-stable mass values upon 1 h. This behavior is related to the different volatility of the solvents (EC and DMC) present in the electrolyte solution. Therefore, the weight decrease detected in the separator membranes is practically ascribed to the evaporation of DMC (boiling temperature equal to 90 °C) instead EC (248 °C) [20]. Weight losses equal to 30 wt.% and 25 wt.% were observed for the PVdF-TrFE (solid squares) and PVDF-HFP (open squares) samples, respectively, after 1 h evaporation whereas only a decrease in weight around 7% was recorded for the PVdF-TrFE/PEO blend (star). This fact is explained by the lower initial content in liquid electrolyte (Table 1) and to stronger interactions of the solution components with PEO.

The ionic conductivity of the PVdF-based electrolyte membranes was determined by impedance spectroscopy measurements taken on symmetric two steel electrode cells at 24 °C and 50 °C, which are represented in Fig. 6 as Nyquist plots. The AC responses, normalized toward the area and the thickness of each sample, show an inclined straight-line (typical of the blocking electrode capacitive behavior) whose intercept with the real axes, Z′, gives the PVdF-based electrolyte membrane ionic resistance [49,50]. At 24 °C the PVdF-HFP electrolyte sample (panel B) exhibits a partial small semicircle (at high frequencies) which does not fall into the origin of the axes. This is likely to be associated to a grain boundary resistance contribution [49,50] as also confirmed by the NLLSQ analysis of the AC responses. At medium temperature (50 °C), a shift of the high frequency intercept inclined straight-line is observed, indicating a decrease of the electrolyte membrane ionic resistance. The ionic conductivity of the PVdF-based electrolyte

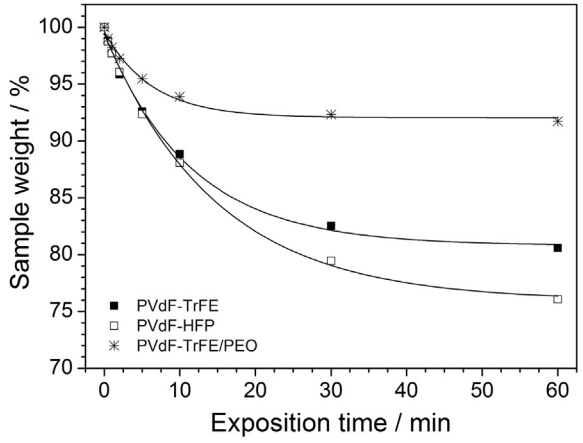


**Fig. 5.** Retention of liquid electrolyte as a function of the exposition time (at room temperature) for $Li^+$-conducting, polymer membranes, based on PVdF-TrFE (panel A), PVdF-HFP (panel B) and PVdF-TrFE/PEO (panel C) hosts, upon swelling in (1 M)$LiPF_6$–EC/DMC(1/1 in weight) electrolyte solution.

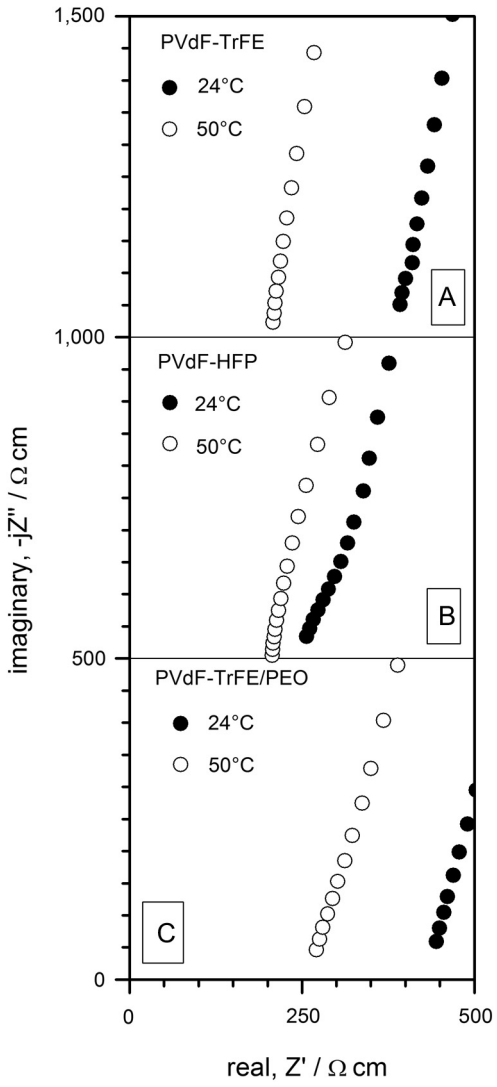


**Fig. 6.** AC response, taken at different temperatures, of $Li^+$-conducting, polymer membranes based on PVdF-TrFE (panel A), PVdF-HFP (panel B) and PVdF-TrFE/PEO (panel C) hosts upon swelling in (1 M)$LiPF_6$–EC/DMC(1/1 in weight) electrolyte solution.

**Table 2**
Comparison among the liquid uptake and ionic conductivity values of the PVdF-based copolymer electrolyte membranes with those of various gel polymer electrolytes reported in literature.

| Polymer host | Electrolyte solution | Liquid content/wt.% | Conductivity/ mS cm$^{-1}$ |
|---|---|---|---|
| PAN[a] | EC–DMC–$LiPF_6$ | 91 | 3.1 (25 °C) |
| PMMA[b] | EC–DMC–$LiN(SO_2CF_3)_2$ | 78 | 0.7 (25 °C) |
| Polyfluorosilicone/ PEO[c] | EC–DMC–$LiPF_6$ | 57 | 1.9 (20 °C) |
| PVdF/CTFE[d] | PC–EC–$LiC(SO_2CF_3)_3$ | 79 | 0.7 (30 °C) |
| PEO[e] | EC–DMC–$LiClO_4$ | 80 | 2.5 (25 °C) |
| PVdF-TrFE | EC–DMC–$LiPF_6$ | 84 | 2.6 (24 °C) |
| PVdF-HFP | EC–DMC–$LiPF_6$ | 81 | 3.5 (24 °C) |
| PVdF-TrFE/PEO | EC–DMC–$LiPF_6$ | 45 | 2.3 (24 °C) |

[a] From Ref. [27].
[b] From Ref. [28].
[c] From Ref. [56].
[d] From Ref. [29].
[e] From Ref. [25].

membranes is depicted in Table 1, which denotes how conduction values above $10^{-3}$ S cm$^{-1}$ are already exhibited at room temperature (24 °C). Also, it is to note that the PVdF-TrFE/PEO blend sample, even if able to retain reduced liquid electrolyte amounts (Table 1), shows conduction values only slightly lower with respect to the PVdF co-polymer electrolytes. This behavior may be ascribed to an optimal pore size and interconnection, thus allowing a better distribution of the liquid electrolyte. In Table 1 are also compared the conduction values determined after dipping the PVdF co-polymer separator membranes in (0.1)LiTFSI–(0.9)$PYR_{14}$TFSI, non-volatile, ionic liquid electrolyte. Conductivities one order of magnitude lower are observed, even still of interest for practical applications ($\geq 10^{-4}$ S cm$^{-1}$) [1–6], mainly attributed to the lower viscosity of the ionic liquid electrolyte with respect the organic one [54].

The physicochemical properties of various gel polymer electrolytes, previously reported in literature, are compared in Table 2 with those of the investigated PVdF-based copolymer electrolyte membranes [25,27–29,56]. The latter show analogous or superior ion conduction values despite comparable liquid uptake values are displayed. This behavior is to be ascribed to weaker interactions between the PVdF copolymer host and the liquid electrolyte (i.e., mainly solvent molecules), thus allowing faster ion transport through the membranes, even if analogous liquid retention is exhibited [25,27–29,56]. It is to note that simpler and cheaper swelling process was adopted for PVdF copolymer with respect to other gel polymer electrolyte systems [25,27–29,56].

The performance of Li/$LiFePO_4$ cathode half-cells, preliminarily investigated in PVdF-HFP electrolyte membranes at room temperature, are reported in Figs. 7 and 8. Panel A of Fig. 7 illustrates the voltage vs. capacity profile of selected discharge half-cycles obtained at various current rates, revealing a well-defined voltage curve typical of $LiFePO_4$ cathodes [55] even at high current densities. A moderate increase in ohmic drop, e.g., from 0.6 V to 0.9 V, is detected with increasing the discharge rates from 0.1C to 2C, this supporting for high conduction of the electrolyte membrane (e.g., high mobility of the $Li^+$ cation). In panel B of Fig. 7 is reported the discharge capacity vs. current rate dependence. A nominal capacity equal to 155 mA h g$^{-1}$ (91.2% of the theoretical value) is delivered, approaching the performance achieved in $LiPF_6$–EC–DMC liquid electrolytes supported by glass fiber separators, (e.g., 155 mA h g$^{-1}$ at 0.1C) [44–46]. It is worth noticing that at 2C (corresponding to 2.0 mA cm$^{-2}$) the cells are still able to deliver above 89% (corresponding to 138 mA h g$^{-1}$) of the capacity (155 mA h g$^{-1}$) discharged at 0.1C (0.1 mA cm$^{-2}$, e.g., at a current density twenty times lower). Such an excellent rate capability, comparable with that

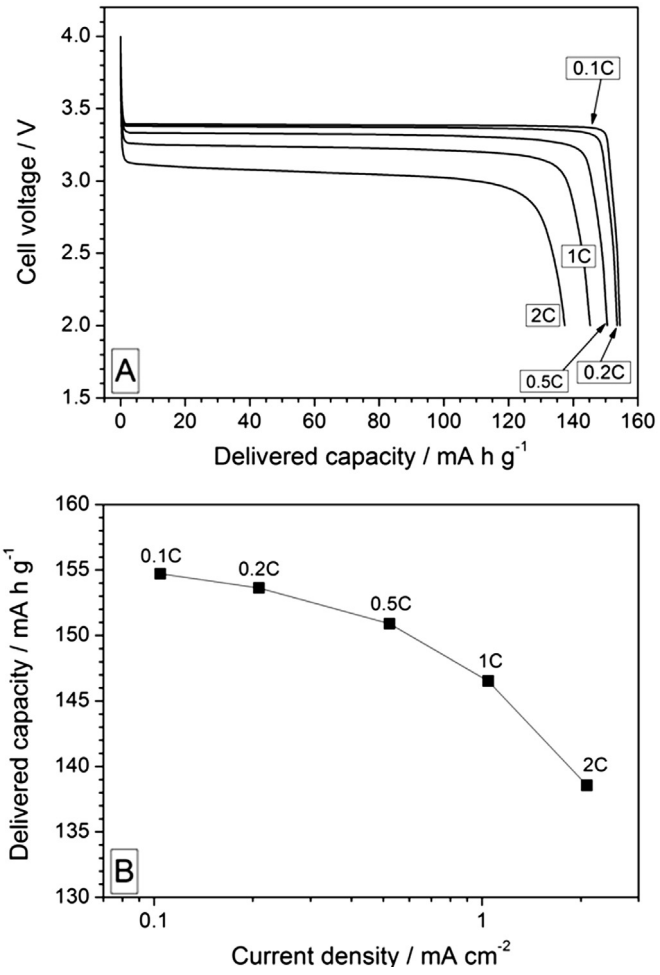


**Fig. 7.** Voltage vs. discharge capacity profiles (panel A) and capacity vs. current density dependence (panel B) of Li/$LiFePO_4$ cathode half-cells containing $Li^+$-conducting, PVdF-HFP separators swollen in (1 M)$LiPF_6$–EC/DMC(1:1 in weight) electrolyte solution. Discharge rate: C/10–2C. Charge rate: C/10. Room temperature.

detected in liquid electrolyte solutions [44–46], supports, once more, for fast transport properties of the PVdF-HFP electrolyte membrane, indicating that negligible diffusive phenomena occur up to 2.0 mA cm$^{-2}$. These promising results suggest that: i) the liquid $LiPF_6$–EC–DMC solution, even if well confined within the

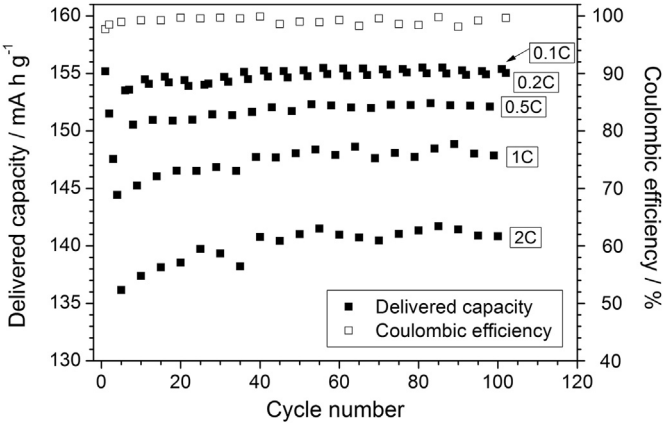


**Fig. 8.** Cycling performance (delivered capacity: solid squares; coulombic efficiency: open squares) of Li/$LiFePO_4$ cathode half-cells containing $Li^+$-conducting, PVdF-HFP separators swollen in (1 M)$LiPF_6$–EC/DMC(1/1 weight) electrolyte solution at room temperature. Discharge rate: C/10–2C. Charge rate: C/10. Room temperature.

PVdF-HFP host, is free to move through the membrane, thus quickly conducting $Li^+$ electrochemically active species; ii) fast ion transport also within the composite cathode (due to adequate and well interconnected pores through the electrode).

The results plotted in Fig. 8 show a very good cycling behavior (delivered capacity: solid squares; coulombic efficiency: open squares) with large capacities even at high current rates (2C) and upon prolonged charge/discharge cycles run at 100% of DOD. For instance, above 99% of the initial capacity is still discharged after 100 cycles run within the full voltage range (100% DOD), thus highlighting an excellent capacity retention. This and the about 100% coulombic efficiency achievements even at high rates and upon prolonged cycling tests (Fig. 8) are certainly related to the very good electrolyte/electrode compatibility, which results from the high purity of the electrolyte materials and the cell manufacturing besides the high stability of the cathode material.

Figs. 9 and 10 illustrate the preliminary performance of Li/Sn–C anode half-cells investigated in PVdF-TrFE electrolyte membranes at room temperature. Panel A of Fig. 9 shows the voltage vs. capacity profiles, typical of tin anodes [44–46], referred to selected discharge half-cycles run at various current rates. A moderate ohmic drop increase, e.g., from 0.7 V to 0.95 V, is recorded with increasing the discharge rates from 0.1C to 2C, once more indicating fast $Li^+$ ion conduction for the PVdF-TrFE electrolyte membrane. In panel B of Fig. 9 is depicted the discharge capacity vs. current density behavior. A nominal capacity equal to 300 mA h $g^{-1}$ is delivered, which is found to decrease with the current rate. Large capacity values are observed up to 0.5C (about 0.8 mA $cm^{-2}$), e.g., 300 mA h $g^{-1}$, 270 mA h $g^{-1}$ and 230 mA h $g^{-1}$ are discharged at 0.1C, 0.2C and 0.5C, respectively. Appreciable capacities (about 140 mA h $g^{-1}$ and 60 mA h $g^{-1}$) are still delivered at higher rates (1C and 2C, respectively). Differently to that recorded for the PVdF-HFP membrane adopted as the electrolyte separator in Li/$LiFePO_4$ cells (e.g., analogous performance with respect to the one observed in $LiPF_6$–EC–DMC solutions), these values are, however, lower than the results observed in liquid electrolyte (e.g., 450 mA h $g^{-1}$ at 0.2C) [44–46], which is to be ascribed to the inferior ion conduction of the PVdF-TrFE polymer electrolyte (2.6 mS $cm^{-1}$ at 24 °C) with respect to the PVdF-HFP (3.5 mS $cm^{-1}$ at 24 °C) membrane (Tables 1 and 2). This behavior, taking also into account that the PVdF-TrFE membranes showed a higher liquid uptake (84 wt.%) with respect to the PVdF-HFP (81 wt.%), is to be ascribed to higher interactions of the PVdF-TrFE host with the $LiPF_6$–EC–DMC solution, thus leading to slower transport properties.

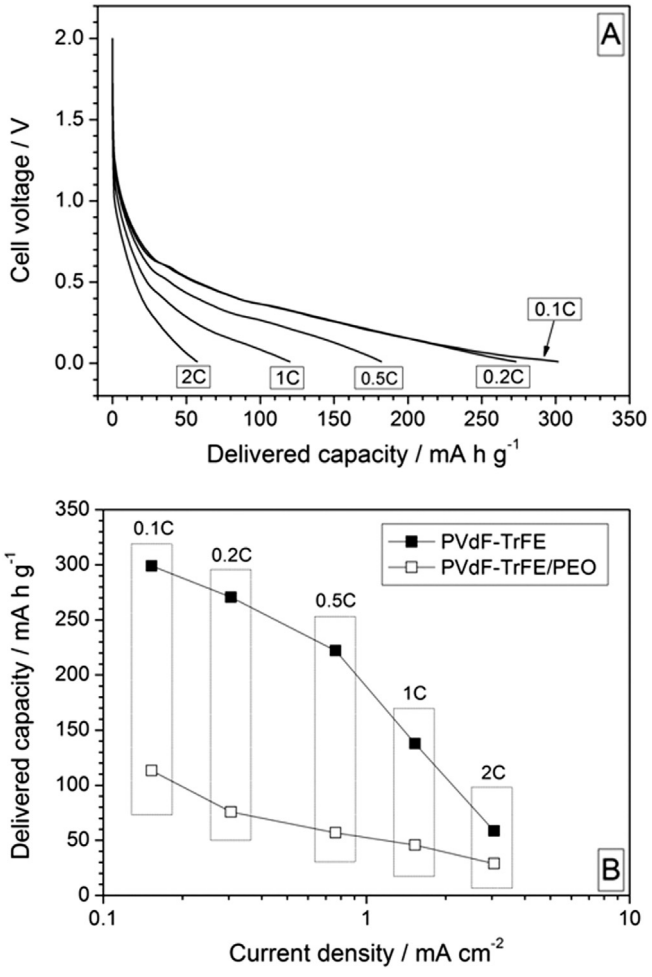


**Fig. 9.** Voltage vs. discharge capacity profiles (panel A) and capacity vs. current density dependence (panel B) of Li/Sn–C anode half-cells containing $Li^+$-conducting, PVdF-TrFE separators swollen in (1 M)$LiPF_6$–EC/DMC(1/1 in weight) electrolyte solution. Discharge rate: C/10–2C. Charge rate: C/10. Room temperature. The rate capability referred to Sn–C anodes in PVdF-TrFE/PEO-based electrolyte membranes is reported in panel B for comparing purpose.

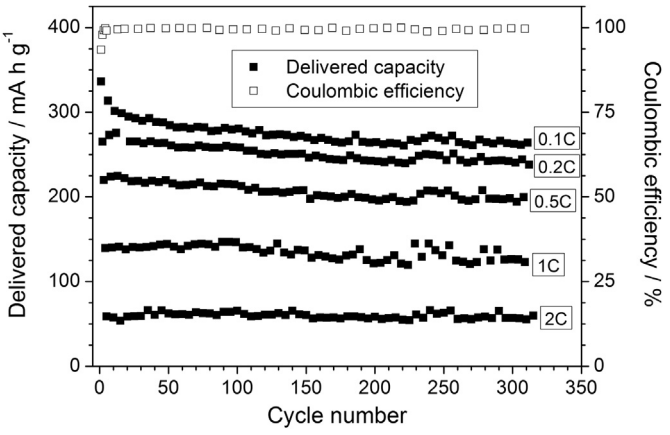


**Fig. 10.** Cycling performance (delivered capacity: solid squares; coulombic efficiency: open squares) of Li/Sn–C anode half-cells containing $Li^+$-conducting, PVdF-TrFE separators swollen in (1 M)$LiPF_6$–EC/DMC(1:1 in weight) electrolyte solution at room temperature. Discharge rate: C/10–2C. Charge rate: C/10. Room temperature.

The data plotted in panel B of Fig. 9 show two well-defined linear trends with a knee at 0.8 mA $cm^{-2}$ (0.5C), due to the delivered capacity limitation originating from different diffusive phenomena taking place in the electrolyte membrane (higher rates) and in the anode active material phase (lower rates). For instance, the value of 0.8 mA $cm^{-2}$ may be taken as the current density limit for the PVdF-TrFE electrolyte separator. The lower rate capability with respect to the Li/$LiFePO_4$ half-cells is likely addressed to the less conductive PVdF-TrFE electrolyte membrane (in comparison to the PVdF-HFP electrolyte separator) and more marked diffusive phenomena within the Sn–C active material (with respect to $LiFePO_4$ [44–46,55]). Finally, the capacity vs. current rate dependence of Li/Sn–C half-cells in PVdF-TrFE/PEO blend electrolyte (open square markers) is reported for comparison purpose. As clearly evidenced from panel B of Fig. 9, reduced capacity values are observed, likely due to the remarkably lower ion conduction of the PVdF-TrFE/PEO membrane (Table 1).

The rate performance of the Li/Sn–C half-cells in PVdF-TrFE electrolyte membrane is also observed in Fig. 10 where are displayed the delivered capacity vs. cycle trend (solid squares) and the coulombic efficiency evolution (open squares) at increasing current rates from 0.1C (0.15 mA $cm^{-2}$) to 2C (3.0 mA $cm^{-2}$) respectively. A

very good cycling behavior is shown even upon prolonged charge/discharge cycles run at 100% of DOD. It is to note that a better capacity retention is observed at high instead at low rates. At 0.1C, upon an initial value equal to 336 mA h $g^{-1}$, the capacity is seen leveling at 300 mA h $g^{-1}$ after 10 cycles and, then, almost linearly decreasing down to 264 mA h $g^{-1}$ upon further 165 consecutive cycles, corresponding to a fade equal to 0.05% per cycle, due to the intrinsic fading of deeply discharged Sn–C anodes [44–46] rather than to PVdF-TrFE electrolyte misbehavior and/or cell design. Conversely, above 99% of the capacity initially delivered at 2C was discharged after 180 cycles, corresponding to a fade lower than 0.002% per cycle. This behavior can be mainly ascribed to the intercalation of the $Li^+$ ion present in the pores of the tin electrodes only. Nominally, no contribution from the $Li^+$ ion diffusion in the bulk electrolyte is existing in this current regime. These results and the leveled 100% coulombic efficiency value even at high current densities and after prolonged tests (Fig. 10) witness very good electrolyte/electrode compatibility, deriving from the high purity of the materials and cell manufacturing.

## 4. Conclusions

The physicochemical properties of electrolyte membranes based on the PVdF-TrFE and PVdF-HFP copolymers, and the PVdF-TrFE/PEO blend, as separators for lithium battery systems, were investigated in organic electrolytes and non-volatile, non-flammable ionic liquid-lithium salt solutions. The results have shown that the examined membranes, particularly those based on the PVdF copolymers, are able to uptake large liquid amounts, e.g., above 80% with respect to the overall weight of the swollen sample, due to their high interconnected porosity (60–70% in volume), leading to ionic conductivity values of the order to $10^{-3}$ S $cm^{-1}$ at room temperature.

Cycling tests performed on Li/$LiFePO_4$ and Li/Sn–C half-cells have revealed very good capacity retention even upon prolonged charge/discharge cycles run at high current rates and 100% of DOD. A capacity fading lower than 0.002% per cycle was observed. Particularly, the Li/$LiFePO_4$ cathode cells have exhibited excellent rate capability, being still able to deliver at 2C above 89% of the capacity discharged at 0.1C. These results, in conjunction with about 100% coulombic efficiency, suggest very good electrolyte/electrode compatibility, which results from the high purity of the electrolyte materials and the cell manufacturing besides the high stability of the electrode active materials.

## Acknowledgments

This work was supported by FEDER through the COMPETE Program and by the Portuguese Foundation for Science and Technology (FCT) in the framework of the Strategic Project PEST-C/FIS/UI607/2011 and grant SFRH/BD/68499/2010 (C.M.C.). The authors thank Solvay for kindly supplying the high quality materials.

## References

[1] P.B. Balbuena, Y. Wang (Eds.), Lithium-ion Batteries: Solid-electrolyte Interphase, Imperial College Press, London, 2004.
[2] G.A. Nazri, G. Pistoia, Lithium Batteries: Science and Technology, Springer, 2009.
[3] M.S. Whittingham, Chemical Reviews 104 (10) (2004) 4271.
[4] B. Scrosati, J. Garche, Journal of Power Sources 195 (9) (2010) 2419.
[5] V. Etacheri, R. Marom, R. Elazari, G. Salitra, D. Aurbach, Energy & Environmental Science 4 (9) (2011) 3243.
[6] C. Daniel, J.O. Besenhard, Handbook of Battery Materials, Wiley, 2012.
[7] A.S. Arico, P. Bruce, B. Scrosati, J.-M. Tarascon, W. van Schalkwijk, Nature Materials 4 (5) (2005) 366.
[8] F. Cheng, J. Liang, Z. Tao, J. Chen, Advanced Materials 23 (15) (2011) 1695.
[9] M. Yang, J. Hou, Membranes 2 (3) (2012) 367.
[10] Y. Xu, Q. Liu, Y. Zhu, Y. Liu, A. Langrock, M.R. Zachariah, C. Wang, Nano Letters 13 (2) (2013) 470.
[11] J. Chen, L. Yang, S. . Fang, S.-i. Hirano, Electrochemistry Communications 13 (8) (2011) 848.
[12] G. Derrien, J. Hassoun, S. Panero, B. Scrosati, Advanced Materials 19 (17) (2007) 2336.
[13] H. Liu, R. Hu, M. Zeng, J. Liu, M. Zhu, Journal of Materials Chemistry 22 (16) (2012) 8022.
[14] L.-X. Yuan, Z.-H. Wang, W.-X. Zhang, X.-L. Hu, J.-T. Chen, Y.-H. Huang, J.B. Goodenough, Energy & Environmental Science 4 (2) (2011) 269.
[15] D. Choi, D. Wang, V.V. Viswanathan, I.-T. Bae, W. Wang, Z. Nie, J.-G. Zhang, G.L. Graff, J. Liu, Z. Yang, T. Duong, Electrochemistry Communications 12 (3) (2010) 378.
[16] G. Wang, H. Liu, J. Liu, S. Qiao, G.M. Lu, P. Munroe, H. Ahn, Advanced Materials 22 (44) (2010) 4944.
[17] P. Arora, Z. Zhang, Chemical Reviews 104 (10) (2004) 4419.
[18] A.M. Stephan, European Polymer Journal 42 (1) (2006) 21.
[19] P. Millet, F. Andolfatto, R. Durand, Journal of Applied Electrochemistry 25 (3) (1995) 233.
[20] K. Xu, Chemical Reviews 104 (10) (2004) 4303.
[21] Y.S. Chung, S.H. Yoo, C.K. Kim, Industrial & Engineering Chemistry Research 48 (9) (2009) 4346.
[22] G. Venugopal, J. Moore, J. Howard, S. Pendalwar, Journal of Power Sources 77 (1) (1999) 34.
[23] B.K. Choi, K.H. Shin, Y.W. Kim, Solid State Ionics 113–115 (0) (1998) 123.
[24] Y. Kang, H.J. Kim, E. Kim, B. Oh, J.H. Cho, Journal of Power Sources 92 (1–2) (2001) 255.
[25] Y. Aihara, G.B. Appetecchi, B. Scrosati, Journal of the Electrochemical Society 149 (2002) A849.
[26] T.-H. Cho, M. Tanaka, H. Onishi, Y. Kondo, T. Nakamura, H. Yamazaki, S. Tanase, T. Sakai, Journal of Power Sources 181 (1) (2008) 155.
[27] G.B. Appetecchi, P. Romagnoli, B. Scrosati, Electrochemistry Communications 3 (2001) 281.
[28] G.B. Appetecchi, F. Croce, B. Scrosati, Electrochimica Acta 40 (1995) 991.
[29] G.B. Appetecchi, F. Croce, A. De Paolis, B. Scrosati, Journal of Electroanalytical Chemistry 463 (1999) 248.
[30] D. Djian, F. Alloin, S. Martinet, H. Lignier, Journal of Power Sources 187 (2) (2009) 575.
[31] C.M. Costa, L.C. Rodrigues, V. Sencadas, M.M. Silva, J.G. Rocha, S. Lanceros-Méndez, Journal of Membrane Science 407–408 (2012) 193.
[32] R. Miao, B. Liu, Z. Zhu, Y. Liu, J. Li, X. Wang, Q. Li, Journal of Power Sources 184 (2) (2008) 420.
[33] J. Saunier, F. Alloin, J.Y. Sanchez, L. Maniguet, Journal of Polymer Science Part B Polymer Physics 42 (12) (2004) 2308.
[34] J. Saunier, F. Alloin, J.Y. Sanchez, B. Barrière, Journal of Polymer Science Part B Polymer Physics 42 (3) (2004) 532.
[35] T. Nakajima, H. Groult, Fluorinated Materials for Energy Conversion, Elsevier Science, 2005.
[36] C.M. Costa, M.M. Silva, S. Lanceros-Mendez, RSC Advances (2013), http://dx.doi.org/10.1039/C3RA40732B.
[37] Z. Jiang, B. Carroll, K.M. Abraham, Electrochimica Acta 42 (17) (1997) 2667.
[38] J. Li, Physical Review Letters 90 (21) (2003) 217601.
[39] C.M. Costa, V. Sencadas, J.G. Rocha, M.M. Silva, S. Lanceros-Méndez, Journal of Solid State Electrochemistry 17 (3) (2013) 861.
[40] C.M. Costa, L.C. Rodrigues, V. Sencadas, M.M. Silva, S. Lanceros-Méndez, Solid State Ionics 217 (0) (2012) 19.
[41] C.M. Costa, J. Nunes-Pereira, L.C. Rodrigues, M.M. Silva, J.L.G. Ribelles, S. Lanceros-Méndez, Electrochimica Acta 88 (0) (2013) 473.
[42] C.M. Costa, M.N.T. Machiavello, J.L.G. Ribelles, S. Lanceros-Méndez, Journal of Materials Science 48 (2013) 3494.
[43] J. Hassoun, D.-J. Lee, Y.-K. Sun, B. Scrosati, Solid State Ionics 202 (1) (2011) 36.
[44] S. Brutti, J. Hassoun, B. Scrosati, C.-Y. Lin, H. Wu, H.-W. Hsieh, Journal of Power Sources 217 (2012) 72.
[45] G.A. Elia, S. Panero, A. Savoini, B. Scrosati, J. Hassoun, Electrochimica Acta 90 (2013) 690.
[46] B. Scrosati, Electrochimica Acta 45 (15–16) (2000) 2461.
[47] B.A. Boukamp, Solid State Ionics 18 (1986) 136.
[48] B.A. Boukamp, Solid State Ionics 20 (1986) 31.
[49] J.R. MacDonald, Impedance Spectroscopy, John Wiley & Sons Editor, New York, 1987.
[50] B.-Y. Chang, S.-M. Park, Annual Review of Analytical Chemistry 3 (1) (2010) 207–229.
[51] A. California, V.F. Cardoso, C.M. Costa, V. Sencadas, G. Botelho, J.L. Gómez-Ribelles, S. Lanceros-Mendez, European Polymer Journal 47 (12) (2011) 2442.
[52] A. Ferreira, J. Silva, V. Sencadas, J.L.G. Ribelles, S. Lanceros-Méndez, Macromolecular Materials and Engineering 295 (6) (2010) 523.
[53] F.M. Gray, Polymer Electrolytes, Royal Society of Chemistry Monographs, Cambridge, 1997.
[54] J.R.D. Rogers, K.R. Seddon, Ionic Liquids: Industrial Application to Green Chemistry. ACS Symposium Series 818, American Chemical Society, Washington, 2002.
[55] N. Ravel, J.B. Goodenough, S. Besner, M. Gauthier, M. Armand, in: Abstracts of the Electrochemical Society and the Electrochemical Society of Japan Meeting (Abstract 127), Honolulu, vol. 99(2), 1997.
[56] G.B. Appetecchi, F. Alessandrini, S. Passerini, G. Caporiccio, B. Boutevin, F. Guida-PietraSanta, Electrochimica Acta 50 (2005) 4396.